The Effects of Covering on Complex Wave Propagation in Gyromagnetic Slotlines

Kuen-Fwu Fuh, *Student Member, IEEE,* and Ching-Kuang C. Tzuang, *Senior Member, IEEE*

Abstract—The evolution of complex leaky waves in partially open gyromagnetic slotlines into complex modes in a shielded slotline is presented. Given a particular stratified gyromagnetic slotline with two sidewalls present, four types (Types I–IV) of guided structures are defined and investigated, depending upon the four possible combinations of top and bottom covers. The behavior of the complex solutions is discussed for the partially open gyromagnetic slotlines. Initially, the slotline of Type I, which lacks both top and bottom covers, shows that no coupling exists among various pairs of leaky waves. By adding only a top cover into Type I, the resultant slotline of Type II exhibits certain coupling between different sets of leaky waves. Similarly, by adding only a bottom cover into Type I, the resultant slotline of Type III shows that certain strong leaky waves of Types I and II now become weak leaky waves. From these numerical experiments, we deduce that the complex modes supported by Type IV, which is completely shielded, can be the result of the mode coupling of the two previously found leaky waves in Types II and III waveguides, respectively. Therefore, the formation of complex modes in shielded slotline is related to the effects of covering on mode coupling of the various leaky waves of the partially open slotlines.

I. INTRODUCTION

RECENTLY many researchers have conducted investigations concerning transmission lines integrated on anisotropic substrates, e.g., [1]–[7]. Among the anisotropic substrates, ferrite is widely used for designing filters, circulators, isolators, scannable antenna, etc. [8]–[11], which are integral components of modern communication equipment. The detailed understanding of the guided properties of those ferrite-loaded waveguides or transmission lines will be beneficial for designing ferrite-based components.

The guided properties of the ferrite-based waveguides and transmission lines can be found in the literature concerning the dominant mode [1], [12], [13], the higher order modes [13], [14], the coupling properties [15]–[17], and the complex modes [3], [18]–[21], etc. Generally, the dominant, higher order, and complex modes are essential constituent elements of the complete mode spectrum of various nonreciprocal closed (boxed) gyromagnetic waveguides. However, the simultaneous existence of the nonspectral forward leaky waves and the spectral backward leaky waves had been reported in [22] for a partially open gyromagnetic slotline without the top cover, of which the eigenvalues of the complex waves are no longer
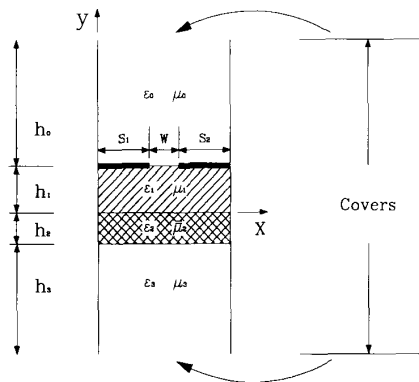
Fig. 1. Four types of nonreciprocal gyromagnetic slotlines are formed by the four possible combinations of placing top and bottom covers. They are Type I (no top and bottom covers), Type II (no bottom cover), Type III (no top cover), and Type IV (shielded structure). Ferrite substrate in Region 2 is magnetized in the x direction. The common structure parameters and material constants for these four types of structures are: $h_1 = h_2 = 1$ mm, $s_1 = s_2 = 1.628$ mm, $w = 0.3$ mm $\epsilon_{0\gamma} = \epsilon_{3\gamma} = 1.0$, $\epsilon_{1\gamma} = \epsilon_{2\gamma} = 12.5$, $4\pi Ms = 4900$ G, and $Ho = 30$ Oe. The other structure parameters that characterize these four structures are: 1) $h_0 = h_3 = \infty$ of Type I, 2) $h_0 = 3.556$ mm and $h_3 = \infty$ of Type II, 3) $h_0 = \infty$ and $h_3 = 1.556$ mm of Type III, and 4) $h_0 = 3.556$ mm and $h_3 = 1.556$ mm of Type IV.

complex-conjugated. The split solutions for the complex waves represent losses in a radiated manner. These complex leaky waves were validated by the transverse field plots showing their forward leaky and backward leaky properties, respectively.

This paper extends the previous work reported in [22], and investigates the progressive evolution of the complex waves controlled by the addition of the covers as shown in Fig. 1. Four types of nonreciprocal gyromagnetic slotlines are defined in Fig. 1, depending on the presence of the top and the bottom covers. Type I has neither top nor bottom covers. Type II (III) contains the top (bottom) cover, while leaving the bottom (top) side open. Type IV contains both top and bottom covers. Types I, II, and III are partially open structures, and they may allow power leakage in the form of parallel-plate waveguide modes. Type IV, however, is constructed in a closed (boxed) manner and no leakage can escape from it. As a result, the conversion of complex leaky waves into bounded complex modes can be deduced by such controlled procedure.

In Section II, the propagation characteristics of the partially open gyromagnetic slotline of Type I will become clear. The effects of adding the top cover to the Type I structure are discussed in Section III. As the guided structure of Type IV

becomes fully closed, the associated complex modes become complex-conjugated. Then Section IV discusses and relates the complex leaky waves of those partially open gyromagnetic slotlines (Types II and III) and the complex modes of the shielded slotline (Type IV). Finally, Section V concludes the paper.

II. GYROMAGNETIC SLOTLINE OF TYPE I

For the purpose of clarity, certain symbols, graphs, and definitions for various types of guided structures under investigation are discussed here. In Fig. 1, the structure parameters and the material constants are given and kept at the same values for all four types of gyromagnetic slotlines, differentiated by the presence of the top and the bottom covers. Fig. 1 also illustrates how Types I–IV structures are defined. The sidewalls at the open sides of Fig. 1 are vertically extended to infinity ($|y| = \infty$), and the full-wave spectral domain approach (SDA) is adopted to analyze these partially open (Types I, II, and III) and closed (Type IV) structures. Although the dispersion characteristics of Types III and IV had already been investigated and reported in [20]–[22], more physical insight can be explored out of detailed analyses of the two partially open structures of Types I and II. Dual axes of opposite polarity are employed in the mode charts to illustrate the nonreciprocal guided properties of the waveguides [20], [21]. The factors $e^{j\omega t}$ and $e^{-j\gamma z}$, where ω is the angular frequency and $\gamma = \beta - j\alpha$, are assumed in our analyses. Throughout the paper, β and α stand for propagation (phase) constant and attenuation constant, respectively. They are plotted by solid lines and dash–dot lines in the mode charts, respectively. The mode charts show only the higher order modes, numbered as four–seven by authors' preference. These higher order modes, however, contain all the important dispersion characteristics in our presentations.

A. The Discussion of Modes Embedded in the Dispersion Characteristics of Type I

In the case of Type I, where neither top nor bottom cover is present, the corresponding dispersion characteristics are plotted in Fig. 2, where prefixes F and B denote forward and backward waves with respect to the positive z direction, respectively. Fig. 2 shows that no mode-coupling effects exist among various designated mode pairs, and the sixth mode pair ($F6$–$B6$) exhibits large spectral gaps. The spectral gaps, which are normally found between the spectral bound and the nonspectral leaky regions [23], exist in all the modal solutions of this paper, regardless of whether they are visible or not. The insets inside Fig. 2 are the most visible ones throughout the paper. In general, the spectral gaps are small in all the particular case studies, and it is hard to differentiate them without an enlarged scale.

As implied in Fig. 2, the higher order modes can be classified by the following different guided-wave behavior. The first region is the bound-wave region, which consists of a pair of forward and backward traveling waves of $\beta/k_0 > 1$ and $\beta/k_0 < -1$, respectively, while $\alpha = 0$. The so-called spectral gap is the second region containing the eigenvalues
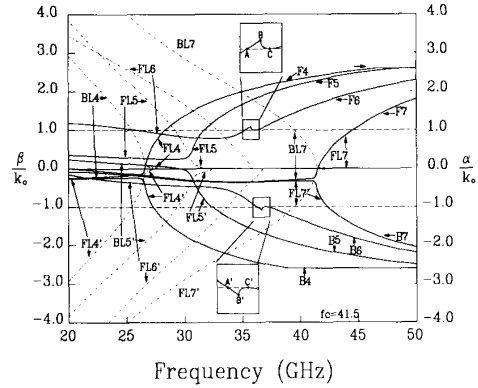

Fig. 2. The dispersion characteristics of the Type I structure defined in Fig. 1. Only four sets of higher order modes numbered from four to seven are presented. The solid lines represent the normalized phase constants β/k_0 and correspond to the vertical axis on the left-hand side. The dash–dot lines represent the normalized attenuation constants α/k_0 and correspond to the vertical axis on the right-hand side. The most visible spectral gaps of the sixth mode pair are enlarged in the insets. Critical points A, B, and C (A', B', and C') are also plotted in the insets and defined in the text.

which cannot be captured by the extreme steepest descent paths in the steepest descent representation of fields [23], [24]. Therefore, they are nonphysical solutions. Since the gyromagnetic slotline is nonreciprocal, the bound waves enter the spectral-gap regions at different frequencies. In addition, there are two different subregions in the spectral gap. One lies in the range with complex γ as being located between two critical points $A(A')$ and $B(B')$ in the insets of Fig. 2. The other is defined between points $B(B')$ and $C(C')$, which contains only real eigenvalues of $|\beta/k_0|$ greater than one, while the corresponding transverse fields grow exponentially. In despite of visible or invisible spectral-gap regions, as frequency is decreased further, sooner or later, a pair of forward leaky waves can be established. They constitute the third type of waves. For example, the backward traveling wave $B7$ leaves the almost invisible spectral-gap region quickly and becomes the forward leaky wave $FL7'$ when frequency is decreased from 45–40 GHz. The $FL7'$ mode conserves the power in such a manner that its electromagnetic fields decay along the negative z direction while increasing in the transverse plane. Because of the nonreciprocity, the pair of two forward leaky waves, e.g., $FL7$ and $FL7'$, does not coincide at the horizontal axis ($\beta = 0$ or $\alpha = 0$). Therefore, as shown in Fig. 2, the $FL7$ mode becomes the backward leaky wave ($BL7$) when the frequency is decreased below the critical frequency $f_c = 41.5$ GHz. When this happens, the sign of the phase constant (β) reverses. Now, the $BL7$ mode remains as the backward leaky wave as frequency is decreased again in Fig. 2. Therefore, we define the fourth region where a pair of nonspectral forward leaky wave and spectral backward leaky wave may coexist. Of importance is the fact that the forward leaky wave (e.g., $FL7'$) and the backward leaky wave (e.g., $BL7$) may couple and result in noncomplex-conjugated pairs of solutions. Furthermore, the corresponding normalized attenuation constants α/k_0 become very large as frequency is decreased. Except for the sixth mode pair, which has no
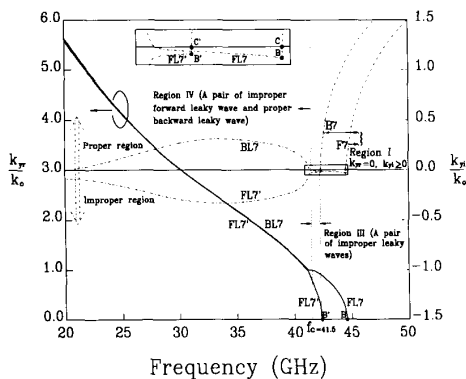
Fig. 3. The frequency-dependent variation of the transverse wavenumber k_{yo} of the seventh mode pair of the Type I structure. The dash–dot lines represent the normalized imaginary parts k_{yi}/k_0 and correspond to the vertical axis on the right-hand side. The solid lines represent the normalized real parts k_{yr}/k_0 and correspond to the vertical axis on the left-hand side. The real parts are always greater than or equal to zero. Therefore, the behavior of each wave type is characterized by the imaginary part. When $k_{yi} > 0$, the wave is proper, and when $k_{yi} < 0$, the wave is improper.

Fig. 4. The dispersion characteristics of the Type II structure defined in Fig. 1. Only four sets of higher-order modes numbered from 4–7 are presented. The solid lines represent the normalized propagation constants β/k_0 and correspond to the vertical axis on the left-hand side. The dash–dot lines represent the normalized attenuation constants α/k_0 and correspond to the vertical axis on the right-hand side. The most visible spectral gaps of the sixth mode pair are enlarged in the insets. Critical points A, B, and C (A', B', and C') are also plotted in the insets and defined in the text.

chance to constitute the backward leaky wave, the fourth and the fifth mode pairs do resemble the seventh pair in every way.

By adding a small portion of dielectric loss in ϵ_1 of Fig. 1, the complex-conjugated solutions for the complex modes of the lossless shielded case [20], [21] now become the noncomplex-conjugated pairs. This indirectly shows that the leaky-wave solutions of Types I, II, and III should be noncomplex-conjugated [25].

B. Transverse Wavenumber $(k_{yo} = k_{yr} - jk_{yi})$ Representation of Various Mode Types

Another view of the various mode types is by means of the transverse wavenumber $k_{yo}(k_{yr} - jk_{yi})$ versus frequency plot. Here, k_{yo} represents the transverse wavenumber of the TM_0 element in the mode spectrum of the parallel-plate waveguide. Referring to Fig. 1, let the field dependence be $e^{-jk_{yo}y}$ and $e^{jk_{yo}y}$ for the upper and lower open air regions, respectively. Thereby, k_{yr} is always greater than or equal to zero. When $k_{yi} > 0$, the solution is proper in the sense that the obtained field solutions decay along positive y and negative y axes. In contrast, when $k_{yi} < 0$, the electromagnetic fields rise to infinity and the complex-wave solution is improper or nonspectral (see Fig. 3 for the proper and improper regions). If the guided-wave structure does leak, the width $(s1+s2+w)$ of the structures defined in Fig. 1 is chosen such that only the TEM mode may leak through the parallel-plate configuration.

Focusing on the particular seventh mode pair of Fig. 2, Fig. 3 plots the corresponding normalized complex transverse wavenumber as a function of frequency using dual axes, the real part (k_{yr}/k_0) on the left-hand side and the imaginary part (k_{yi}/k_0) on the right-hand side. The $F7–B7$ pair has solutions purely positive imaginary; thus, the associated modes are bounded and spectral. Although the spectral gaps of the $F7–B7$ pair are extremely small in Fig. 2, the subregions of the spectral gaps between critical points $B(B')$ and $C(C')$, as shown in Fig. 3, almost line up vertically and become
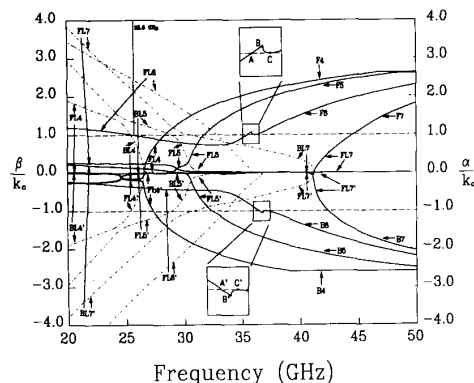
visible. However, the subregions between critical points $A(A')$ and $B(B')$ are still hard to differentiated. Thus, points A and A' are not shown in Fig. 3. Immediately to the left of the two vertical lines representing the spectral gaps are the nonspectral (improper) solutions for the $FL7–FL7'$ pair. One of them, namely, the $FL7$ mode, becomes the spectral (proper) backward leaky wave when the operating frequency is below $f_c = 41.5$ GHz. Fig. 3 clearly shows that the complex solutions represent leaky losses and are not complex-conjugated as both real parts and imaginary parts are not equal in magnitude.

III. DISPERSION CHARACTERISTICS OF TYPE II

A. The Effects of Top Cover

By adding a top cover to Type I at $y = h_0 + h_1$, Fig. 1 becomes a Type II structure. Its dispersion characteristics are plotted in Fig. 4. When we compare Figs. 4 and 2, the dispersion characteristics of the $BL7–FL7'$ pair of Fig. 2 are altered significantly by the addition of the top cover. The $F6–B6$ and $FL6–FL6'$ modes of Fig. 2, however, are influenced only very slightly. No mode coupling exists between the sixth and seventh mode pairs in Fig. 4. As shown in Fig. 4, when the frequency is further decreases, however, the $BL7–FL7'$ modes couple to the $FL5–BL5'$ modes and $BL4–FL4'$ modes. When one set of a forward leaky wave and a backward leaky wave couples to another set, they couple in a manner very similar to the mode coupling of the complex modes for the shielded structure (i.e., Type IV) [20], [21].

We may illustrate such a mode-coupling mechanism between the multiple sets of complex leaky waves by overlaying the $BL4–FL4'$ and the $FL5–BL5'$ of Fig. 2 on the $BL4–FL4'$, $BL5'–FL5$, and $BL7–FL7'$ of Fig. 4. The results are shown in Fig. 5, where the dash–dot lines and solid lines are the direct replica of the corresponding modes of Figs. 4 and 2, respectively. By simply connecting the dash–dot
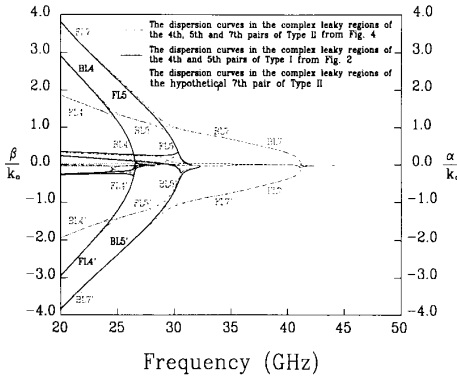
Fig. 5. The dispersion curves (solid lines) of the fourth and fifth mode pairs of the Type I structure in their complex-leaky region are superimposed to the dispersion curves (dash–dot lines) of the fourth, fifth, and seventh mode pairs of the Type II structure. The dotted curves are added to represent the hypothetical seventh mode pair of the Type II structure before mode coupling takes place.

Fig. 6. The frequency-dependent variation of the transverse wavenumber k_{yo} of the sixth mode pair of the Type II structure. The dash–dot lines represent the normalized imaginary parts k_{yi}/k_0 and correspond to the vertical axis on the right-hand side. The solid lines represent the normalized real parts k_{yr}/k_0 and correspond to the vertical axis on the left-hand side. The real parts are always greater than or equal to zero. There is no backward leaky wave in this mode pair when the bottom cover is absent.

lines via dotted lines as shown in Fig. 5, the picture of mode coupling as reported in [21, Figs. 3 and 7] starts to emerge. While the imaginary parts of the coupled complex leaky waves repel each other, the real parts cross. Therefore, after mode coupling due to the presence of top cover, $BL7(FL7')$ becomes $FL7(BL7')$ and $FL5(BL5')$ becomes $BL5(FL5')$, and so on. Detailed analyses of the data shown in Fig. 4 enable us to designate the modes as shown in Figs. 4 and 5. Furthermore, we may view the dotted curves of Fig. 5 as the modal solutions of the uncoupled $BL7–FL7'$ modes. Since the leaky wave solutions of Type I never couple as shown in Fig. 2, it is plausible to conclude that the $BL7–FL7'$ modes couple to the $BL4–FL4'$ modes and $FL5–BL5'$ modes for the particular case study with top cover present.

B. The Wave Properties of the Sixth Mode Pair

The sixth mode pairs of Types I and II guided structures deserve special attention. As shown in Figs. 2 and 4, when frequency decreases from 50 to 20 GHz, the mode conversion process is summarized as follows. It begins with $F6–B6$ (forward traveling and backward traveling waves), then two visible spectral gaps, and finally $FL6–FL6'$ (two forward leaky waves). The $FL6–FL6'$ pair covers a fairly large frequency spectrum, and they do not couple. Therefore, no backward leaky wave is found in this mode pair for the particular case study. Such observation can also be clearly seen by plotting the transverse wavenumber of the sixth mode pair versus frequency. As illustrated in Fig. 6, to the left of the spectral-gap regions, two nonspectral improper forward leaky-wave solutions exist since their imaginary parts are negative real.

Detailed analyses, which map the complex solutions of the $FL6–FL6'$ modes into the steepest descent plane, show that all of the leaky solutions of the $FL6'$ mode are captured, whereas those of the $FL6$ mode below 25.6 GHz are not captured. Those complex solutions not captured in the steepest descent plane are not physical and correspond to the solutions with $|\beta/k_0|$ greater than 1 [26]. Accordingly, Figs. 4
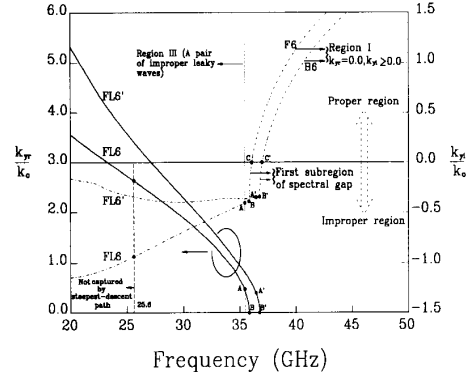
and 6 mark the regions for the nonphysical $FL6$ solutions, respectively.

IV. FROM LEAKY WAVES TO COMPLEX MODES

A. The Sixth Mode Pair in Type III

The effects of adding the top cover on the spectral gaps and leakage of the sixth mode pair of Type I structure, in which no covers are present, are illustrated in Fig. 7. The dispersion curves of the sixth mode pairs of Types I and II structures are plotted in Fig. 7 from 34–38 GHz. Dispersion curves of Types I and II structures are distinguished by various lines types. Based on Fig. 7, one can recognize that the top cover has very little effect on the sixth mode pair whether the modes are bounded ($F6–B6$) or leaky ($FL6–FL6'$). From the discussion presented in Section III-B, the $FL6–FL6'$ modes will leaky for a fairly wide spectrum. Since the top cover has almost negligible effects on the leaky $FL6–FL6'$ modes, we are left with only one option which will affect the leaky modes, i.e., the addition of the bottom cover. Fig. 8, showing the dispersion characteristics of the Type III structure with top cover opened and bottom cover closed, manifests the fact that the $FL6–FL6'$ modes of Types I or II now strongly couple to each other and result in a pair of forward leaky wave $FL6$ and backward leaky wave $BL6'$. Based on the analyses of Figs. 2, 4, and 8, the sixth mode pair predominantly leaks into the bottom region. When the bottom cover is added while leaving the top cover open, the leaky wave may bounce back from the bottom plate and leak into the top open region weakly.

In summary, the existence of $FL6–BL6'$ modes in Type III implies a fairly small amount of energy leakage. The $BL7–FL7'$, $FL6–BL6'$, $BL5–FL5'$, and $FL4–BL4'$ are all alike. When watching these modes closely, they resemble waveguide modes below cutoffs [27]. Thus, the energy associated with the excitation of these modes is mostly reactive.
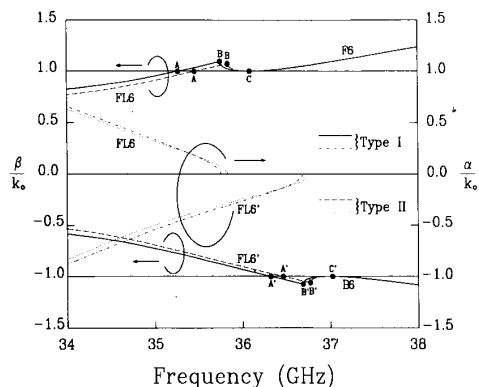
Fig. 7. Comparison of the enlarged spectral gaps of the sixth modal pairs shown in Figs. 2 and 4, respectively. The solid line and the dash–dot line designate the normalized phase constants β/k_0 and attenuation constants α/k_0 of the sixth mode pair of the Type I structure defined in Fig. 1. The dashed line and the dotted line designate the normalized phase constants β/k_0 and attenuation constants α/k_0 of the sixth mode pair of the Type II structure defined in Fig. 1.

Fig. 9. The dispersion curves of the seventh mode pair of the Type II structure (solid lines) and the sixth mode pair of the Type III structure (dashed lines) are superimposed to illustrate the mode coupling invoked by the existence of the top and bottom covers. The resultant solutions of complex modes of the shielded Type IV structure are also included and plotted in dash–dot lines.
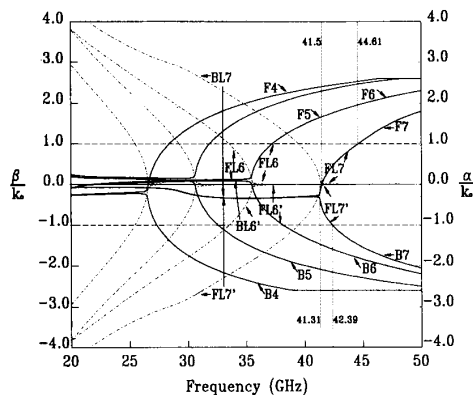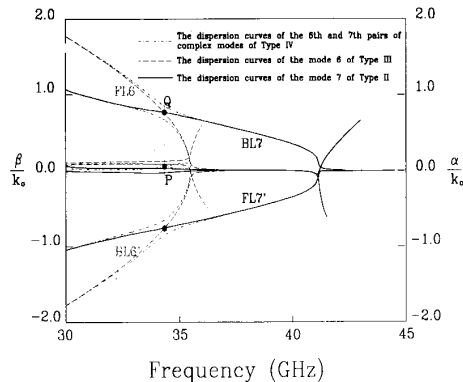

Fig. 8. The dispersion characteristics of the Type III structure defined in Fig. 1. Only four sets of higher order modes numbered from 4–7 are presented. The solid lines represent the normalized propagation constants β/k_0 and correspond to the vertical axis on the left-hand side. The dash–dot lines represent the normalized attenuation constants α/k_0 and correspond to the vertical axis on the right-hand side. The sixth mode pair now can support the backward leaky wave $BL6'$.

B. Leaky Waves and Complex Modes

By adding a top cover to the Type III structure, a Type IV guided structure is established. Recognizing the fact that the top cover has a strong influence on the seventh mode pair (see Section III-A), while the bottom plate has a large impact on the sixth mode pair, we superimpose the dispersion curves (in solid lines) of the seventh pair of Type II and those (in dashed lines) of the sixth pair of Type III; the resultant dispersion characteristics are shown in Fig. 9. These two sets of curves cross for the imaginary part. If we further superimpose the full-wave solutions of complex modes of the sixth and seventh orders of Type IV, i.e., the shielded structure, the picture of the mode-coupling mechanism between modes six and seven emerges very clearly [20], [21]. We may view mode seven of Type II and mode six of Type III as the so-called hypothetical

modes as defined in [20], [21]. Notice that mode seven of Type II and mode six of Type III have absorbed most of the covering effects before the guided structure is fully shielded. Therefore, the Type IV structure only perturbs these two modes slightly. As a result, the complex leaky waves are converted to complex modes by placing top and bottom covers one after another.

V. CONCLUSION

A progressive change of complex leaky waves in a gyromagnetic slotline with and without top or bottom covers is presented. Four types of gyromagnetic slotlines (Types I–IV) are thus defined and their dispersion characteristics are discussed in detail. While the mode charts of these guided-wave structures show similar spectral gaps as reported earlier in [23], the coexistence of a pair of nonspectral (improper) forward leaky waves and/or the coexistence of a pair of nonspectral forward leaky wave and spectral backward leaky wave are newly found and reported in the partially open nonreciprocal gyromagnetic transmission lines. Of more interest is that the action of adding the top and bottom covers results in mode coupling among complex leaky waves. At the authors' preference, four sets of modes numbered as 4, 5, 6, and 7 are defined. Initially, the Type I structure of no top and bottom covers shows no mode-coupling phenomenon between various sets of leaky waves (see Fig. 2). With only a top cover present, the Type II structure shows that the seventh mode pair is strongly affected by the top cover, and it couples to modes in the fourth and fifth sets while showing no coupling to modes in the sixth pair (see Figs. 4 and 5). The sixth mode pair behaves quite differently from other sets of modes in Types I and II structures. It shows that only a pair of forward leaky waves can exist when it leaks (see Figs. 2, 4, and 6). With only a bottom cover present, however, the sixth mode pair now can support a pair of forward leaky wave and backward leaky wave (see Fig. 8). We deduce that modes in the sixth pair predominantly leak into the bottom air region and are strongly influenced by the bottom cover. Separately choosing

the two sets of strongly influenced modes by the top and bottom covers, namely, the seventh pair of Type II and the sixth pair of Type III, we show that these two sets of modes constitute the so-called hypothetical modes [20], [21], which yield two pairs of complex modes after the mode-coupling mechanism invoked by the addition of top and bottom covers that result in a lossless shielded guided structure of Type IV (see Fig. 9). Perhaps one of the fruitful areas of application of the presented data is antenna design. For example, it is possible to excite modes in the regions where only forward leaky waves can exist since they exhibit very small attenuation constants (see Figs. 2, 4, and 8).

REFERENCES

[1] M. Geshiro and T. Itoh, "Analysis of double-layered finlines containing magnetized ferrite," *IEEE Trans. Microwave Theory Tech.*, vol. MTT-35, pp. 1377–1381, Dec. 1987.

[2] E. El-Sharawy and R. W. Jackson, "Coplanar waveguide and slot line on magnetic substrates: Analysis and experiment," *IEEE Trans. Microwave Theory Tech.*, vol. 36, pp. 1071–1079, June 1988.

[3] R. Marqués, F. L. Mesa, and M. Horno, "Nonreciprocal and reciprocal complex and backward waves in parallel plate waveguides loaded with a ferrite slab arbitrary magnetized," *IEEE Trans. Microwave Theory Tech.*, vol. 41, pp. 1409–1418, Aug. 1993.

[4] M. Tsuji, H. Shigesawa, and A. A. Oliner, "Printed-circuit waveguides with anisotropic substrates: A new leakage effect," in *1989 IEEE MTT-S Int. Microwave Symp. Dig.*, pp. 783–786.

[5] M. Geshiro, S. Yagi, and S. Sawa, "Analysis of slotlines and microstrip lines on anisotropic substrates," *IEEE Trans. Microwave Theory Tech.*, vol. 39, pp. 64–69, Jan. 1991.

[6] T. Kitazawa and T. Itoh, "A asymmetrical coplanar waveguide with finite metallization thickness containing anisotropic substrate medium," *IEEE Trans. Microwave Theory Tech.*, vol. 39, pp. 1426–1433, Aug. 1991.

[7] Y. Chen and B. Beker, "Spectral-domain analysis of open and shielded slotlines printed on various anisotropic substrates," *IEEE Trans. Microwave Theory Tech.*, vol. 41, pp. 1872–1877, Nov. 1993.

[8] A. Beyer and K. Solbach, "A new fin-line ferrite isolator for integrated millimeter-wave circuits," *IEEE Trans. Microwave Theory Tech.*, vol. MTT-29, pp. 1344–1348, Dec. 1981.

[9] D. Hahn, "Exact calculation of partial-height waveguide Y-junction circulator using mode-matching techniques," *Electron. Lett.*, vol. 24, pp. 966–968, July 1988.

[10] J. Uher, J. Bornemann, and F. Arndt, "Magnetically tunable rectangular waveguide E-plane integrated circuit filters," *IEEE Trans. Microwave Theory Tech.*, vol. 36, pp. 1014–1022, June 1988.

[11] H. Maheri, M. Tsutsumi, and N. Kumagai, "Experimental studies of magnetically scannable leaky-wave antennas having a corrugated ferrite slab/dielectric layer structure," *IEEE Trans. Antenn. Propagat.*, vol. 36, pp. 911–917, July 1988.

[12] T. Kitazawa, "Analysis of shielded striplines and finlines with finite metallization thickness containing magnetized ferrites," *IEEE Trans. Microwave Theory Tech.*, vol. 39, pp. 70–74, Jan. 1991.

[13] J. C. Minor and D. M. Bolle, "Modes in the shielded microstrip on a ferrite substrate transversely magnetized in the plane of the substrate," *IEEE Trans. Microwave Theory Tech.*, vol. MTT-19, pp. 570–577, July 1971.

[14] W. Zieniutycz, "Modes of propagation in slot line with layered substrate containing magnetized ferrite," *Electron. Lett.*, vol. 19, pp. 135–136, Feb. 1983.

[15] I. Awai and T. Itoh, "Coupled-mode theory analysis of distributed nonreciprocal structures," *IEEE Trans. Microwave Theory Tech.*, vol. MTT-29, pp. 1077–1086, Oct. 1981.

[16] D. B. Sillars and L. E. Davis, "Analysis of nonreciprocal coupled image lines," *IEEE Trans. Microwave Theory Tech.*, vol. MTT-35, pp. 629–635, July 1987.

[17] J. Mazur and M. Mrozowski, "On the mode coupling in longitudinally magnetized waveguiding structures," *IEEE Trans. Microwave Theory Tech.*, vol. 37, pp. 159–165, Jan. 1989.

[18] C.-K. C. Tzuang, C.-Y. Lee, and J.-T. Kuo, "Complex modes in lossless nonreciprocal finline," *Electron. Lett.*, vol. 26, no. 22, pp. 1919–1920, 1990.

[19] R. Marqués, F. Mesa, and M. Horno, "On the complex nature of higher order modes in lossless nonreciprocal transversely magnetized waveguides," *IEEE Microwave and Guided Wave Lett.*, vol. 2, pp. 278–280, July 1992.

[20] C.-K. C. Tzuang and J. M. Lin, "Mode-coupling formation of complex modes in a shielded nonreciprocal finline," in *1991 IEEE MTT-S Int. Microwave Symp. Dig.*, pp. 571–574.

[21] ———, "On the mode-coupling formulation of complex modes in a nonreciprocal finline," *IEEE Trans. Microwave Theory Tech.*, vol. 41, pp. 1400–1408, Aug. 1993.

[22] C.-K. C. Tzuang, K.-F. Fuh, and M. Mrozowski, "Complex leaky waves of a partially open nonreciprocal slotline on gyromagnetic substrate," in *1994 IEEE MTT-S Int. Microwave Symp. Dig.*, pp. 1693–1696.

[23] P. Lampariello, F. Frezza, and A. A. Oliner, "The transition region between bound-wave and leaky wave ranges for a partially dielectric-loaded open guiding structure," *IEEE Trans. Microwave Theory Tech.*, vol. 38, pp. 1831–1836, Dec. 1990.

[24] T. Tamir and A. A. Oliner, "Guided complex waves," *Proc. IEE*, vol. 110, pp. 310–334, Feb. 1963.

[25] M. Mrozowski, Dept. Electron., Technical Univ. Gdańsk, Gdańsk, Poland, private communication.

[26] A. A. Oliner, "Leakage from higher modes on microstrip line with application to antennas," *Radio Sci.*, vol. 22, pp. 907–912, Nov. 1987.

[27] C. T. Tai, "Evanescent modes in a partially filled gyromagnetic rectangular waveguide," *J. Appl. Phys.*, vol. 31, pp. 220–221, 1960.

Kuen-Fwu Fuh (S'92) was born in Taiwan on May 14, 1966. He received the B.S. degree in electronic engineering from the Tamkang University, Taipei, Taiwan, in 1989 and the M.S. degree in communication engineering from the National Chiao Tung University, Hsinchu, Taiwan, in 1991, where he is currently working toward the Ph.D. degree.

His research interests include the development of field theory of ferrite-loaded waveguides and planar circuits and microwave and millimeter-wave integrated circuit design.

Ching-Kuang C. Tzuang (S'84–M'86–SM'92) was born in Taiwan on May 10, 1955. He received the B.S. degree in electronic engineering from the National Chiao Tung University, Hsinchu, Taiwan, in 1977, the M.S. degree from the University of California at Los Angeles in 1980, and the Ph.D. degree in electrical engineering from the University of Texas at Austin in 1986, where he worked on high-speed transient analyses of monolithic microwave integrated circuits.

From February 1981–June 1984, he was with TRW, Redondo Beach, CA, working on analog and digital monolithic microwave integrated circuits. Since September 1986, he has been with the Institute of Communication Engineering, National Chiao Tung University, Hsinchu, Taiwan. His research activities involve the design and development of millimeter-wave and microwave active and passive circuits and the field theory analysis and design of various quasi-planar integrated circuits.